Theoret. chim. Acta (Berl.) 5, 379—397 (1966)

Commentationes

Low Spin Ferric Hemoglobin Complexes

Gilda Harris

Hansen Laboratory of Biophysics, Stanford University, Stanford, California

Received April 12, 1966

A calculation has been made of the energy eigenfunctions and eigenvalues of low spin ferric ion in complexes with a strong cubic crystal field including the effects of tetragonal and rhombic distortions and of spin-orbit coupling among the ground state components and with excited states. Using the resultant, spin-orbit coupled eigenfunctions as a basis set, the magnetic susceptibility, the components of magnetic field energy, and the lattice and valence contributions to an electric field gradient at the iron nucleus were all calculated as a function of rhombic, tetragonal, and spin-orbit coupling strength used as parameters: R, u and δ. All of the calculated results agree reasonable well with experiment for the values of parameters $R = 1000\ \mathrm{cm}^{-1}$, $u = 2000\ \mathrm{cm}^{-1}$ and the free ion value $\delta = 420\ \mathrm{cm}^{-1}$. These values of parameters were selected for the excellent fit they gave of the calculated values of g_x, g_y and g_z compared with the experimental ones obtained from single crystal electron spin resonance of ferrihemoglobin azide. With them, a value of 2.29 Bohr magnetons was calculated for the effective magnetic moment compared to the experimental value of 2.35. The total field gradient calculated under the same conditions, predicts a nuclear quadrupole moment Q in the range of $.107 - .127$ Barns, which is smaller than the range predicted from the high spin ferric ion results. Reasons for this discrepancy are discussed.

Ausgehend von einem starken kubischen Ligandenfeld und unter Berücksichtigung tetragonaler (R) und rhombischer (u) Verzerrung sowie der Spin-Bahn-Kopplung (δ) werden Eigenfunktionen und Energien für ‚Low-Spin'-Ferrihämoglobinkomplexe berechnet. Mit den Parametern $R = 1000\ \mathrm{cm}^{-1}$, $u = 2000\ \mathrm{cm}^{-1}$, $\delta = 420\ \mathrm{cm}^{-1}$ erhält man für Suszeptibilität, elektrischen Feldgradienten am Fe und g-Werte gute Übereinstimmung mit experimentellen Daten. Aus dem berechneten Feldgradienten folgt ein Quadrupolmoment des Fe^{57} von 0.107—0.127 Barn, im Gegensatz zu den viel höheren Resultaten bei ‚High-Spin'-Fe(III)-Verbindungen; diese Diskrepanz wird diskutiert.

Les fonctions propres et les énergies du complexe Ferrihémoglobine «low spin» sont calculées pour un fort champ de ligandes à symétrie cubique, en tenant compte des distortions tétragonale (R) et rhomboédrique (u), ainsi que du couplage spin-orbite (δ). Avec les paramètres $R = 1000\ \mathrm{cm}^{-1}$, $u = 2000\ \mathrm{cm}^{-1}$, $\delta = 420\ \mathrm{cm}^{-1}$, on trouve pour la susceptibilité, le gradient du champ électrique à l'emplacement de Fe et le facteur g des valeurs en bon accord avec les données expérimentales. On déduit du gradient de champ calculé un moment quadrupolaire de Fe^{57} de 0,107 à 0,127 Barn, en désaccord avec les résultats beaucoup plus élevés obtenus à partir des associations Fe (III) «high spin». Ce désaccord fait l'objet d'une discussion.

I. Indroduction

Ferric ion with a $3d^5$ configuration has a ${}^6S$ ground state in the free ion and many excited quartet and doublet states. When it becomes part of a complex molecule depending on the strength and symmetry of the crystal field, it is possible for a quartet or a doublet state more stabilized by the field than the ground state to become the ground state. Such a change in spin state is most directly manifested by the observed values of effective magnetic moment associated with the ferric ion. This rather striking property is illustrated by ferric ion in a series of related ferrihemeproteins. Depending on the nature of the sixth ligand, a spectrum of effective magnetic moments have been measured [1, 2, 3] ranging from the five electron, spin only value of 5.92 to the single electron value of 1.73 (see Tab. 1). Such sixth ligands as H_2O and F^- ion leave ferric ion in a sextet ground state, with N_3^- and CN^- it is in a doublet state with a finite contribution of orbital angular momentum to the measured magnetic moment. For such ligands as OH^- the ground state of the ferric ion is neither doublet or sextet. Similarly, if the sixth ligand is kept fixed and the nature of the ring or protein varied slightly, again a change in spin state is observed (see Tab. 2).

Table 1. *Effective Magnetic Moments of Ferric Ion in Hemoglobin Derivatives*

	μ_{eff}		
Ligand	Ref. [1]	Ref. [2]	Ref. [3]
F^-	5.76	5.92	5.92
H_2O	5.65	5.80	5.84
$HCOO^-$	5.44		
OCN^-	5.40		
SCN^-	5.06		
OH^-	4.66	5.11	
NO_2^-	4.13		
$SeCN^-$	3.88		
Imidazole	2.87		
CN^-	2.50	2.50	
Azide$^-$	2.35	2.84	2.84
SH^-	2.26		

Table 2. *Effect of Change in Heme Protein on Ferric Ion Magnetic Moment* [2]

Ferriheme-Hydroxide	
Hemoglobin	5.11
Myoglobin	4.47
Peroxidase	2.66
Cytochrome C	2.14
Ferriheme-Azide	
Catalase	5.36
Hemoglobin	2.84; (2.35 [1])

In all of these compounds, the field strengths and symmetries must be close to the spin-transition region, because small changes in these conditions are enough to make the ground state of the ferric ion a sextet state, a doublet state, or be somewhere in between. Also, since these low spin states lie rather high in energy above the ground state in the free ion, such ease of transfer is an indication of strong fields in these complexes.

Other experimental evidence gives us further clues about the field strength and local field symmetries. Single crystal electron spin resonance of the high spin H_2O and F^- derivaties of ferrihemoglobin [3] points to a local tetragonal symmetry with one g value in the plane of the ring nitrogens and another perpendicular to it. For the low spin azide derivatives three distinct g values have been measured [3], indicating a rhombic distortion of the field symmetry. Both high and low spin derivatives have Mössbauer resonance spectra of Fe^{57} which split by the interaction of the nuclear quadrupole moment with a nonvanishing electric field gradient at the nucleus. The magnitude of this splitting is about 2—4 times that in other ferric ion complexes, another indication of the strong electric fields in these complexes. A Mössbauer resonance doublet is observed in both tetragonal and rhombic symmetry.

Calculations

The six-fold degenerate ${}^6A_1$ ground state of the high spin complexes is unaffected by a crystal field of any symmetry. Nor is there spin-orbit coupling interaction among its member states. Yet the results of magnetic susceptibility measurements, Mössbauer resonance and electron spin resonance indicate a zero field splitting of these states into three doubly degenerate partners and a non-spherically symmetric charge distribution of these states. To possibly explain these properties, for the high spin system it is necessary to invoke spin-orbit coupling of the sextet ground state with excited, non-spherically symmetric electronic states resulting in a splitting into three doublet states $^6A_1$ (± 1/2), (± 3/2), and (± 5/2). Such a calculation was made in strong crystal fields of D_4 symmetry including more and more excited states until the addition of others did not change the nature of the ground and low lying electronic states which determine most of the properties of interest of the system [*4*].

Table 3. *Basis Set of States Used in O and D_4 Symmetry*

O_h State	O_h Config.	D_4 State	D_4 Configuration	Energy of States Electrostatic	O_h	D_4
$^6A_1$	$t_2^3(^4A_2)\ e^2(^3A_2)$	$^6A_1$	$b_2\ e_1\ e_2(^4B_1)\ b_1\ a_1(^3B_1)$	0	0	0
$^4T_1$	$t_2^4(^3T_1)\ e(^2E)$	$^4A_2$	$b_2^2\ e_1\ e_2(^3B_2)\ b_1(^2B_1)$	$10\ B + 6\ C$	$-\Delta$	$-4u/3$
		^4E	$b_2\ e_1^2\ e_2(^3E)\ b_1(^2B_1)$	$10\ B + 6\ C$	$-\Delta$	$-u/3$
$^4T_2$	$t_2^4(^3T_1)\ e(^2E)$	$^4B_2$	$b_2^2\ e_1\ e_2(^3A_2)\ b_1(^2B_1)$	$18\ B + 6\ C$	$-\Delta$	$-4u/3$
		^4E	$b_2\ e_1^2\ e_2(^3E)\ b_1(^2B_1)$	$18\ B + 6\ C$	$-\Delta$	$-u/3$
$^2A_2$	$t_2^4\ (^1E)\ e(^2E)$	$^2B_1$	$b_2^2\ e_1^2\ (\mathrm{s}A_1)\ b_1(^2B_1)$	$12\ B + 9\ C$	$-\Delta$	$-4u/3$
$^2T_1$	$t_2^4\ (^3T_1)\ e(^2E)$	$^2A_2$	$b_2^2\ e_1\ e_2(^3B_2)\ b_1(^2B_1)$	$13\ B + 9\ C$	$-\Delta$	$-4u/3$
		^2E	$b_2\ e_1^2\ e(^3E)\ b_1(^2B_1)$	$13\ B + 9\ C$	$-\Delta$	$-u/3$
$^2T_2$	$t_2^4(^1T_2)\ e(^2E)$	$^2B_2$	$b_2^2\ e_1^2(^1A_2)\ b_1(^2B_1)$	$17\ B + 9\ C$	$-\Delta$	$-4u/3$
		^2E	$b_2\ e_1^2\ e(^3E)\ b_1(^2B_1)$	$17\ B + 9\ C$	$-\Delta$	$-u/3$
$^2T_2$	$t^5(^2T_2)$	$^2B_2$	$b_2\ e_1^2\ e_2^2(^2B_2)$	$15\ B + 10\ C$	-2Δ	$+2/3u$
		^2E	$b_2^2\ e_1^2\ e(^2E)$	$15\ B + 10\ C$	-2Δ	$-u/3$
^2E	$t_2^4(^1A_1)\ e(^2E)$	$^2B_1$	$b_2^2\ e_1^2(^1A_1)\ b_1(^2B_1)$	$22\ \mathrm{B} + 9\ C$	$-\Delta$	$-4u/3$
		$^2A_1$	$b_2^2\ e_1^2(^1A_1)\ a_1(^2A_1)$	$22\ B + 9\ C$	$-\Delta$	0
$^2T_1$	$t_2^4(^1T_2)\ e(^2E)$	$^2A_2$	$b_2^2\ e_1^2(^1B_2)\ b_1(^2B_1)$	$23\ B + 9\ C$	$-\Delta$	$-4u/3$
		^2E	$b_2\ e_1^2\ e(^1E)\ b_1(^2B_1)$	$23\ B + 9\ C$	$-\Delta$	$-u/3$
$^2T_2$	$t_2^4(^3T_1)\ e(^2E)$	$^2B_2$	$b_2^2\ e_1\ e_2(^3A_2)\ b_1(^2B_1)$	$27\ B + 9\ C$	$-\Delta$	$-4u/3$
		^2E	$b_2\ e_1^2\ e_2(^3E)\ b_1(^2B_1)$	$27\ B + 9\ C$	$-\Delta$	$-u/3$
$^2A_1$	$t_2^4(^1E)\ e(^2E)$	$^2A_1$	$b_2^2\ e^2(^1B_1)\ b_1(^2B_1)$	$32\ B + 9\ C$	$-\Delta$	$-4u/3$
^2E	$t_2^4(^1A_1)\ e(^2E)$	$^2B_1$	$b_2\ e_1^2(^1A_1)\ b_1(^2B_1)$	$31\ B + 12\ C$	$-\Delta$	$-4u/3$
		$^2A_1$	$b_2^2\ e_2^2(^1A_1)\ a_1(^2A_1)$	$31\ B + 12\ C$	$-\Delta$	0

With a strong crystal field of cubic symmetry, the original $3d^5$ configuration becomes a set of five $t_2^n\ e^{5-n}$ configurations. Forty three 5-electron multiplet states can then be built from these strong field configurations. These states are the strong field analogues of the free ion terms and are labeled by a total spin and symmetry representation i.e. $|\ Sh\rangle$ quantum number. We have allowed twelve of the lowest strong cubic field states to interact. These become 21 states when further split by a tetragonal field. The set of states used, together with their electrostatic and crystal field energies to first order, are listed in Tab. 3. The states of a given multiplet can further be labeled by their z component of spin and by the component of the representation to which they belong, i.e. each state is labeled by the four quantum numbers $|\ ShM_s\theta\rangle$. When this is done, the original set of 12 strong cubic field $|\ Sh\rangle$ multiplets turns out to be a total of 66 states, which factor into two degenerate 15×15 and 18×18 spin-orbit coupling matrices in tetragonal symmetry. These blocks of states may also be labeled by the representation t and components τ to which they belong in the spinor group D_4^*. The list of 66 basis states in the $| ShM_s\theta\rangle$ scheme factored according to $| t\tau\rangle$ is given in Tab. 4. After spin-orbit coupling then, there are 33 pairs of Kramers doublets. A detailed description of the calculation of the spin-orbit elements, resulting eigenvalues and eigenfunctions, and other properties of interest for the high spin system with this basis set, will be presented elsewhere [*4*].

We have already used the results of this calculation to explain with reasonable success the observed properties of the high spin systems [*5*]. The high spin system is defined as the field strength region where the ground state is predominantly the $^6A_1$ $(-1/2)$ component. This is true for cubic fields $\leq$ 25000 cm^{-1} with tetragonal distortions of 1000 – 5000 cm^{-1}. All of the high spin properties were assigned with field parameters for which this condition was true, but which were close enough to the transition region i.e. $>$ 25000 cm^{-1} to make it reasonable that a change in one ligand could push the system to the low spin side.

Table 4. *Basis set in* $| ShM_s\theta\rangle$ *scheme*[a]

	$E'\alpha'$		$E'\beta'$		$E''\alpha''$		$E''\beta''$
5	$^6A_1$ (1/2)	6	$^6A_1$ $(-1/2)$	1	$^6A_1$ (5/2)	2	$^6A_1$ $(-5/2)$
				4	$^6A_1$ $(-3/2)$	3	$^6A_1$ (3/2)
9	$^4T_1$ (0, 1/2)	10	$^4T_1$ $(0, -1/2)$				
14	$^4T_1$ $(1, -1/2)$	17	$^4T_1$ $(-1\ +1/2)$	8	$^4T_1$ $(0, -3/2)$	7	$^4T_1$ (0, 3/2)
15	$^4T_1$ $(-1, 3/2)$	12	$^4T_1$ $(+1, -3/2)$	11	$^4T_1$ (1, 3/2)	16	$^4T_1$ $(-1, -3/2)$
				18	$^4T_1$ $(-1, -1/2)$	13	$^4T_1$ (1, 1/2)
20	$^4T_2$ $(0, -3/2)$	19	$^4T_2$ (0, 3/2)				
23	$^4T_2$ (1, 3/2)	28	$^4T_2$ $(-1, -3/2)$	21	$^4T_2$ (0, 1/2)	22	$^4T_2$ $(0, -1/2)$
30	$^4T_2$ $(-1, -1/2)$	25	$^4T_2$ $(+1, +1/2)$	26	$^4T_2$ $(1, -1/2)$	29	$^4T_2$ $(-1, 1/2)$
				27	$^4T_2$ $(-1, 3/2)$	24	$^4T_2$ $(1, -3/2)$
33	$^2T_1$ (0, 1/2)	34	$^2T_1$ $(0, -1/2)$				
				31	$^2A_2$ $(i, 1/2)$	32	$^2A_2$ $(i, -1/2)$
36	$^2T_1$ $(1, -1/2)$	37	$^2T_1$ $(-1, 1/2)$				
				38	$^2T_1$ $(-1, -1/2)$	35	$^2T_1$ (1, 1/2)
44	$^2T_2$ $(-1, -1/2)$	41	$^2T_2$ (1, 1/2)				
				39	$^2T_2$ (0, 1/2)	40	$^2T_2$ $(0, -1/2)$
48	$^2T_2$ $(-1, -1/2)$	45	$^2T_2$ (1, 1/2)	42	$^2T_2$ $(1, -1/2)$	43	$^2T_2$ $(-1, 1/2)$
53	^2E $(\theta, 1/2)$	54	^2E $(\theta, -1/2)$	46	$^2T_2$ $(1, -1/2)$	47	$^2T_2$ $(-1, 1/2)$
				49	$^2T_2$ (0, 1/2)	50	$^2T_2$ $(0, -1/2)$
60	$^2T_2$ $(-1, -1/2)$	57	$^2T_2$ (1, 1/2)				
				51	^2E $(\varepsilon, 1/2)$	52	^2E $(\varepsilon, -1/2)$
61	$^2A_1$ $(i, 1/2)$	62	$^2A_1$ $(i, -1/2)$				
				55	$^2T_2$ (0, 1/2)	56	$^2T_2$ $(0, -1/2)$
65	^2E $(\theta, 1/2)$	66	^2E $(\theta, -1/2)$				
				58	$^2T_2$ $(1, -1/2)$	59	$^2T_2$ $(-1, 1/2)$
				63	^2E $(\varepsilon, 1/2)$	64	^2E $(\varepsilon, -1/2)$

We have also shown how and under what conditions the transition to a low spin ground state occurs and the nature of the transition region. Near the boundary of the high spin system region, the $^6A_1$ $(-3/2)$ state becomes the dominant component of the ground state. The transition to a double ground state occurs by the mixing into the sextet ground state of more and more doublet character until over a range of about 1000 cm^{-1}, the ground state is a pure doublet. The intermediate spin system then, occuring approximately between 26000 and 27000 cm^{-1} in cubic field strengths, is characterized by a substantially mixed sextet-doublet ground

---

[a] Numbering of states is in order of 1st order electrostatic and crystal field and spin-orbit coupling energies.

state. The expected properties of ferric ion in this region will be discussed elsewhere.

The results of our calculations show that it is the ${}^2T_2(t_2^5)$ excited state that becomes the ground state at cubic fields greater than about 27000 cm^{-1}, for spin-orbit coupling parameters in the range 150 – 600 cm^{-1} and tetragonal field strengths of 1000 – 5000 cm^{-1}. The particular component of this state which mixes strongly with the ${}^6A_1$ ($\pm$ 3/2) states and finally becomes the ground state is a ${}^2T_2(\pm 1, \mp 1/2)$ doublet, i.e. state 46 and 47 of the E'', α'' and β'' 18 basis function set.

For the low spin system then, in D_4^* symmetry, the same calculation as for the high spin system, including excited states, was continued but for cubic field strengths higher than 27000 cm^{-1}. These results then should be applicable to low spin systems with tetragonal symmetry. However, unlike high spin systems, we know that there is evidence of rhombic fields in the only low spin ferric hemoglobin derivative whose single crystal electron spin resonance has been obtained, i.e. three distinct g values for the azide [*3*]. Therefore we also wish to extend our consideration for the low spin case to rhombic fields.

Before doing this however, in order to determine the elaborateness of the calculation necessary to reasonably explain observed properties, we wish to consider the question of whether or not for the low spin system one needs to include excited state interactions, as was necessary for the high spin system. This question is quite relevant, since unlike the high spin ${}^6A_1$ ground state, the ${}^2T_2$ state is affected both by the crystal field and by spin-orbit coupling among its degenerate partners to first order. Since there are now present these first order effects which are absent in the high spin system, the question arises as to whether higher order interactions of the same kind are appreciable. To answer this question, a calculation of the spin-orbit coupling among only the six ${}^2T_2(t_2^5)$ states of the ground state multiplet in D_4 symmetry was made. The details of this calculation are given in the next section. It is then followed by a comparison with the results of the more elaborate machine calculation including excited states, in order to evaluate the effect of excited state addition. We then proceed to a calculation of spin-orbit coupling in a rhombic field among the six low spin ground state components. From these new energies and eigenfunctions we calculate such properties as components of the magnetic field energies, the effective magnetic moment of the ferric ion, and components of the electric field gradient. These results are compared with experiment and previous calculations whenever possible. Finally we compare high and low spin results and point out the success and limitations of the crystal field explanation of these two systems.

II. Spin Orbit Coupling of ${}^2T_2$ Ground State Components in Tetragonal Symmetry

A. First Order Energies

The ${}^2T_2(t_2^5)$ strong cubic field state is six-fold degenerate with a first order electrostatic and cubic crystal field energy of $15B + 10C - 2\Delta$ relative to the ${}^6A_1(t_2^3e^2)$ state as shown in Tab. 3. The six states can be labeled in the $| ShM_S\theta >$ scheme as shown in Tab. 5. In this labeling, complex components $\theta = (1, 0, -1)$ of the T_2 representation are used. If spin-orbit coupling is to be considered, it is also convenient to work in a spinor representation $| Sht\tau >$ in which the spin-orbit coupling operator is diagonal. Tab. 5 also shows the six ${}^2T_2$ states labeled by the spinor representation E' or E'' and component α or β of the D_4^* group.

The ${}^2T_2$ state is split into two states by a tetragonal field as shown in Fig. 1, a doubly degenerate ${}^2B_2$ state and a four-fold degenerate ${}^2E$ state. These have a total energy separation μ which is defined as the tetragonal field strength. First order spin-orbit coupling within these states further splits the ${}^2E$ state into two doubly degenerate states, one belonging to the E' and the other to the E'' representation of D_4^*. The energy separation between these two states is δ which is the spin-orbit coupling strength parameter. Thus, even to first order, the ${}^2T_2$ sextet is split by spin-orbit coupling in a tetragonal field into three doubly degenerate components as shown in Fig. 1. The first order energies relative to the unsplit ${}^2E$ states are given also in Tab. 5. The zero field splitting among these three states to first order then is $\Delta E_1 = \delta$ and $\Delta E_2 = \mu - 1/2\ \delta$. The spin-orbit coupling strength is typically of the order of 400 and the value of μ is about 2000 cm^{-1}. Thus the magnitude of the zero field splitting in the low spin compounds is approximately 400 and 1600 cm^{-1} as compared to 5 – 20 cm^{-1} for the high spin system. We see then that first order effects alone are about two orders of magnitude greater than the total effect of 30 excited states on the high spin ground state.

Table 5. *Basis Set for Low Spin System: Ground State Only*

$O_h(ShM\theta)$	$D_4(Sh)$	$D_4^*(t\tau)$	D_4^* Energy[a] (first order)	One Hole Notation[b]	$\Phi_i(i)$
${}^2T_2(1, -1/2)$	${}^2E$	$E''\alpha''$	$-\delta/2$	$\|1\alpha\rangle$	1
${}^2T)(-1, 1/2)$	${}^2E$	$E''\beta''$	$-\delta/2$	$\|-1\beta\rangle$	1′
${}^2T_2(-1, -1/2)$	${}^2E$	$E'\alpha'$	$+\delta/2$	$\|-1\alpha\rangle$	2
${}^2T_2(1, 1/2)$	${}^2E$	$E'\beta'$	$+\delta/2$	$\|1\beta\rangle$	2′
${}^2T_2(0, 1/2)$	${}^2B_2$	$E''\alpha''$	$+\mu$	$\|\zeta\beta\rangle$	3
${}^2T_2(0, -1/2)$	${}^2B_2$	$E''\beta''$	$+\mu$	$\|\zeta\alpha\rangle$	3′

[a] Relative to $E({}^2E) = 0$; δ = spin-orbit coupling parameter; μ = tetragonal field strength parameter.

[b] Following Griffith, J. Nature **180**, 30 (1957).

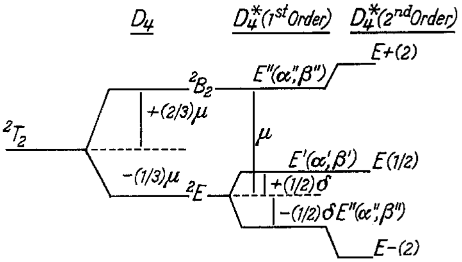

Fig. 1. Splitting of Low Spin Ground State of Ferric Ion in D_4 Symmetry

B. Second Order Spin-Orbit Mixing of ${}^2T_2$ Components

Two of the three doubly degenerate components of the ${}^2T_2$ state belong to the same representation in D_4^*, i.e. $t = E''$, and hence mix under spin-orbit coupling. These two are: the ground state partner of the ${}^2E$ state and the ${}^2B_2$ doublet. The middle ${}^2E$ component belongs to $E'(\alpha', \beta')$ and remains unmixed with the other two in D_4^* symmetry. Thus to the approximation of considering only the six components of the ${}^2T_2$, the solution of the problem of spin-orbit coupling in tetragonal symmetry involves the solution of a 2×2 $E''(\alpha'', \beta'')$ matrix and a 1×1 $E'(\alpha', \beta')$ matrix. The energies of the two mixed doubly degenerate states are the roots of the quadratic:

$$E_\pm = \tfrac{1}{2}\left[-(\delta/2 - \mu) \pm \sqrt{(\delta/2 - \mu)^2 + 2\delta(\delta + \mu)}\right].$$

Thus the first order energy of the ground state is lowered and the energy of the ${}^2B_2$ component is raised, as shown in Fig. 1. The energy of the middle component remains at $\delta/2$. The difference in diagonal matrix elements $H_{22} - H_{11}$ is $(\mu + \delta/2)$. Therefore, for a given value of spin-orbit coupling strength, the stronger the tetragonal field the less the interaction between these two states (see Tab. 6). The off-diagonal element of spin-orbit coupling is $\delta/\sqrt{2}$ and hence for a given value of tetragonal field strength the greater the value of spin-orbit coupling the greater the interaction. This may also be seen in Tab. 6.

Table 6. *First and second order energies of the three $^2T_2$ ground state components*[a]

		2nd order energies			1st order energies		% change in energy	zero field splitting	
	μ[d]	$E_-(2)$	$E_{1/2}$	$E_+(2)$	$E_-(1)$	$E_+(1)$	of E_+	ΔE_1[b]	ΔE_2[c]
δ[e] = 420	200	−366	210	356	−210	200	78.0	576	146
	300	−346	210	436	−210	300	45.3	556	226
	500	−318	210	608	−210	500	21.6	528	398
	1000	−279	210	1069	−210	1000	6.9	+489	859
	2000	−249	210	2039	−210	2000	2.0	+459	1829
	3000	−237	210	3027	−210	3000	0.9	+447	2817
	4000	−230	210	4020	−210	4000	0.5	+440	3810
δ = 300	300	−234	210	384	−150	300	28.0	384	234
	3000	−164	210	3014	−150	3000	0.47	314	2864

[a] All units are in cm^{-1}.

[b] ΔE_1 = first energy interval $E(^2E\ E'') - E(^2E\ E')$.

[c] ΔE_2 = second energy interval $E(^2B_2\ E'') - E(^2E\ E')$.

[d] μ = tetragonal field strength.

[e] δ = spin-orbit coupling parameter (free ion value: 420).

C. Ground State Properties

The three doubly degenerate components with energies E_-, $E_{\frac{1}{2}}$, E_+ are:

$$\Psi_1(\alpha'', \beta'') = A\Phi_{1(1')} + B\Phi_{3(3')}$$

$$\Psi_2(\alpha', \beta') = \Phi_{2(2')}$$

$$\Psi_3(\alpha'', \beta'') = B\Phi_{1(1)} - A\Phi_{3(3')} .$$

Since, as seen from Tab. 6, the zero-field splitting is very large, most of the properties of the system will be determined by the nature of the lowest lying $^2T_2$ component Ψ_1. In particular, the observed electron spin resonance behavior of the system is the behavior of this state.

When a magnetic field is turned on, the double degenerate ground state is split into two components: $E''\alpha''$ and $E''\beta''$. The z component of the magnetic field does not mix these two states. The difference in the z magnetic field energies of each partner is:

$$\Delta E = g_z \beta H_z$$

where

$$g_z = \langle \beta'' \mid L_z + 2S_z \mid \beta'' \rangle - \langle \alpha'' \mid L_z + 2S_z \mid \alpha'' \rangle .$$

For this mixed ground state

$$g_z = 2\,|(2A^2 - B^2)| .$$

The x and y component of the magnetic field does mix the two degenerate partners $E''\alpha''$ and $E''\beta''$ of the ground state. There is no diagonal element of magnetic field energy in these directions. Therefore the total energy separation between these two states in an x or y magnetic field is twice the off-diagonal matrix element

$$g_{\perp} = 2\,\langle {}^2T_2E''\alpha'' \mid L_x + 2S_x \mid {}^2T_2E''\beta''\rangle\,.$$

With this mixed ground state wave function, resulting from spin-orbit interaction in D_4 symmetry:

$$g_x = g_y = g_{\perp} = 2\,\left|(\sqrt{2}\,AB + B^2)\right|\,.$$

Thus, as usual for tetragonal symmetry, even with spin-orbit coupling, there are two distinct g values.

We have calculated values of A, B, g_z, and $g_{\perp}$ for selected values of μ. These are given in Tab. 7.

Table 7. *D_4^* Ground State Functions: Comparison of Results with and without Excited States*[a]

μ	3000	1000	500	300	200
A	.995	.967	.939	.909	.805
A'	.987	.967		$-.901$	$-.878$
B	$+.090$	.232	$-.342$	$-.416$	$-.441$
B'	$+.094$	$-.232$		$+.422$	.467
g_{11}	3.92	3.646	3.30	2.95	2.83
g'_{11}		3.66		2.90	2.66
g_1	0.270	0.742	1.141	1.416	1.61
g'_1				1.32	1.48
ΔE_1	447	489	528	556	576
$\Delta E'_1$	481	517		587	607
ΔE_2	2817	859	398	226	146
$\Delta E'_2$	2710	849		224	144

[a] $\Delta = 28000$, $\delta = 420$. All energy units are in cm^{-1}. Primed values are results including excited states, unprimed values are ground-state results.

III. Effect of Excited State Mixing on Low Spin Ground State Properties in D_4^*

We now wish to examine the effect on the zero field splitting and nature of the ground state wave function of allowing excited states to mix with the components of the ${}^2T_2$ ground state. As a continuation of the high spin calculation, the most elaborate basis set shown in Tab. 4 included 30 excited states belonging to E' and E'' representations of D_4^*, in addition to the three doubly degenerate ground state components. The zero field splittings ΔE_1 and ΔE_2 obtained from a diagonalization of the 15×15 E' matrix and the 18×18 E'' matrix are given in Tab. 7, together with the mixing coefficients and g-values. We see that, while there are noticeable differences, the results are close enough that, to describe the properties of the system in general, one would not make much of an error to consider only the ground state functions in the case of the low spin systems.

As soon as excited states are also included in the calculation, the results would be somewhat dependent on the cubic field strength, since this quantity enters in the intermultiplet energy differences. Tab. 8 shows the effect of the cubic field strength on the coefficients of mixing of the two $^2T_2E''$ states into the ground state, at a fixed value of μ and δ. A slight decrease of mixing occurs with increasing field, but again this is a very small effect because the entire effect of the excited state mixing is small compared to the ground state interaction. In addition, we know that the spin systems are very close to the minimum spin transition conditions in the ferriheme complexes and we do not have much freedom in the value of cubic field strength to assign low spin properties.

To compare either set of results with experiment, one needs an example of a low spin ferric hemoglobic complex in a local crystal electric field of tetragonal symmetry. The Mössbauer resonance splitting has been observed for three low spin compounds, the N_3^-, CN– and CO derivatives [6]. However, both tetragonal and rhombic symmetry give a doublet with different contributions to the magnitude of the observed splitting. The single crystal electron spin resonance has been done for only one of these, the azide. The three distinct g values are: $g_z = 2.80$, $g_x = 1.72$ and $g_y = 2.22$ [3]. Obviously, we cannot get two different in-plane g values from D_4 symmetry. However, the expression for g_z is the same in rhombic and D_4 symmetry, if one considers only the contributions from the $^2T_2$ components. The closest comparison with experimental low spin results that can be made with the calculated results from D_4^* symmetry is then to fit the data to the observed g_z value. The best fit to the experimental g_z value is for a $\mu = 200$ cm^{-1} with a $\delta = 420$ cm^{-1}. The expression for $g_\perp$ is 5% lower than g_x and about 30% lower than g_y.

Table 8. *Effect of cubic field strength on mixing of two $^2T_2(E'')$ components in low spin ground state*[a]

Δ	28000	30000	35000	40000	excited states not included
A'	−.9874	−.9913	−.9940	−.9948	−.995
B'	+.0942	+.0938	+.0931	+.0926	+.090

[a] $\mu = 3000$, $\delta = 420$. Energy unit is cm^{-1}.

If we were to end out investigations at this point we would conclude that the low spin system has a somewhat higher overall cubic field than the high spin systems, i.e. > 27000 compared to $20 - 24000$ cm^{-1}, but has a much smaller tetragonal distortion, i.e. 200 cm^{-1} *vs* $3000 - 5000$, for the high spin system. This is not too bad a qualitative picture, if we recall that the azide, for example, is a complex with the sixth ligand also a nitrogen. Its bonding then, might be more similar to the in-plane nitrogen bonding and stronger than the H_2O and F– bonding. This would lead to a stronger cubic field strength and less tetragonal distortion.

However, we wish to more precisely characterize the magnetic field results and make a quantitative calculation of the electric field gradient components to try to explain the observed Mössbauer resonance splitting and also to calculate the magnetic susceptibility of the azide. To do all this, with the most physically reasonable model, we proceed to a consideration of the interaction of the components of the ${}^2T_2(t_2^5)$ state, under spin-orbit coupling in a rhombic field. What we have established thus far is that it is reasonable to ignore the effects of excited states.

IV. Spin-Orbit Interaction in Rhombic Crystal Fields

A. Energy Matrix

If we allow a rhombic distortion of the crystal field, the one electron orbital splitting of the triply degenerate t_2 state is shown in Fig. 2 for a real component basis set:

$$t_{2g}(\eta) = \sqrt{3}\, d_{xz} = \quad t_{2g}(y) = \quad -\sqrt{2}\,(d_1 - d_{-1}) \tag{1a}$$

$$t_{2g}(\xi) = \sqrt{3}\, d_{yz} = \quad i \cdot t_{2g}(x) = \quad i/\sqrt{2}\,(d_1 + d_{-1}) \tag{1b}$$

$$t_{2g}(\zeta) = \sqrt{3}\, d_{xy} = 1/i \cdot t_{2g}(z) = 1/i \cdot \sqrt{2}\,(d_2 - d_{-2})\,. \tag{1c}$$

The corresponding rhombic field diagonal matrix elements are then:

$$< t_{2g}(\eta) \mid V_R \mid t_{2g}(\eta) > = \quad R/2\,(d_{xz}) \tag{2a}$$

$$< t_{2g}(\xi) \mid V_R \mid t_{2g}(\xi) > = -R/2\,(d_{yz}) \tag{2b}$$

$$< t_{2g}(\zeta) \mid V_R \mid t_{2g}(\zeta) > = \quad 0 \quad (d_{xy})\,. \tag{2c}$$

Thus for positive μ, the d_{xy} orbital lies below the d_{xz}, d_{yz} pair and for positive R the d_{yz} orbital energy is lower than the d_{xz} orbital energy. For a five electron (t_2^5) state or equivalently a one-hole state with this same basis set, the order of energies is inverted.

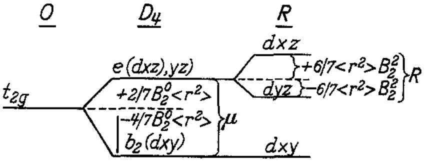

Fig. 2: t_{2g}-1 Electron Orbital Splitting in Rhombic Symmetry

We wish now to transform to the basis set we have been using, the six functions listed in Tab. 5 with complex components. Doing this, we find that the rhombic field component mixes the ${}^2T_2(1)$ components with the ${}^2T_2(-1)$, i.e. $< {}^2T_2^*(1) \mid V_R \mid {}^2T_2(-1) > = + R/2$, thus mixing the two states ${}^2E\ E''(\Phi_1)$ and ${}^2E\ E'(\Phi_2)$ which did not mix under spin-orbit coupling.

If we introduce spin-orbit coupling and a rhombic field at the same time, we no longer have a $2 \times 2\ E''$ matrix and $1 \times 1\ E'$ matrix each with its degenerate partner, but now there are two degenerate 3×3 matrices, each of the following form:

$$\begin{array}{c|ccc} & \Phi_1 & \Phi_2 & \Phi_3 \\ \hline \Phi_1 & -\delta/2 - E & R/2 & \delta/\sqrt{2} \\ \Phi_2 & R/2 & \delta/2 - E & 0 \\ \Phi_3 & \delta/\sqrt{2} & 0 & \mu - E \end{array} \tag{3}$$

in the basis set defined and labeled in Tab. 5.

B. Ground State Functions and Properties

The ground state is now a mixture of all three components, being linked to one, ${}^2E\ E'$, by the rhombic distortion and to the other, ${}^2B_2E''$, by spin-orbit coupling. The three mixed final states have the form:

$$\Psi_1(\Psi'_1) = A_{11}\Phi_1 + B_{13}\Phi_3 + C_{12}\Phi_2\,, \tag{4a}$$

$$\Psi_2(\Psi'_2) = A_{21}\Phi_1 + B_{23}\Phi_3 + C_{22}\Phi_2\,, \tag{4b}$$

$$\Psi_3(\Psi'_3) = A_{31}\Phi_1 + B_{33}\Phi_3 + C_{32}\Phi_2\,. \tag{4c}$$

This set of functions differs from those in tetragonal symmetry in that the ground state and third state in D_4^* has $C = 0$, and the second state is pure Φ_2.

With this form of ground state function, the g values, without allowing the magnetic field to mix states to higher than first order, are:

$$g_z = 2\,|\,2A^2 - B^2\,|\,, \tag{5a}$$

$$g_y = 2\,|\,(-\sqrt{2}\,A + B)\,(\sqrt{2}\,C + B)\,|\,, \tag{5b}$$

$$g_x = 2\,|\,(\sqrt{2}\,A - B)\,(\sqrt{2}\,C - B)\,|\,. \tag{5c}$$

The first order contribution to the total effective magnetic moments is:

$$\mu^2_{\text{eff}}(1) = \{\sum_N [\mathscr{H}_z^2(N, N) + \mathscr{H}_y^2(N, N'') + \mathscr{H}_x^2(N, N'')]\cdot \exp(-E_N/kT)\}\times$$
$$\times\{\sum_N \exp(-E_N/kT)\}^{-1} \tag{6a}$$

and the second order terms are:

$$+\,2kT\left\{\sum_N\left[\sum_M \frac{\mathscr{H}_z^2(N,M) + \mathscr{H}_y^2(N,M) + \mathscr{H}_x^2(N,M)}{E_M - E_N}\right]\cdot\exp(-E_N/kT)\right\}\times$$
$$\times\{\sum_N \exp(-E_N/kT)\}^{-1} \tag{6b}$$

where the operator $\mathscr{H}_i = (L_i + 2S_i)$ and N, N'' are degenerate partners.

For the off-diagonal matrix elements of the magnetic field energies which appear in the second order contributions, a general expression for the magnetic field energies is used to take into account differences in coefficients in each wave function N, M:

$$H_z(N, M) = (2A_N A_M - B_N B_M)\,, \tag{7a}$$

$$H_y(N, M) = \tfrac{1}{2}(-\sqrt{2}\,A_N + B_N)(\sqrt{2}\,C_M + B_M) + $$
$$+\,\tfrac{1}{2}(-\sqrt{2}\,A_M + B_M)(\sqrt{2}\,C_N + B_N)\,, \tag{7b}$$

$$H_x(N, M) = \tfrac{1}{2}(\sqrt{2}\,A_N - B_N)(\sqrt{2}\,C_M - B_M) + $$
$$+\,\tfrac{1}{2}(\sqrt{2}\,A_M - B_M)(\sqrt{2}\,C_N - B_N)\,. \tag{7c}$$

When $C = 0$, $H_x = H_y$ and the rhombic results go over to the tetragonal. If only the ground state contributes to the magnetic moment, e.g. Eq. (6) reduces to

$$\mu^2_{\text{eff}} = (\tfrac{1}{2}g_x)^2 + (\tfrac{1}{2}g_y)^2 + (\tfrac{1}{2}g_z)^2 +$$
$$+\,2kT\sum_{M=1}^{2}[H_z^2(0, M) + H_y^2(0, M) + H_x^2(0, M)]/E_M \tag{8}$$

where $E_1 = \Delta E_1$, $E_2 = \Delta E_2$.

The valence contribution to the electric field gradient components from any two degenerate partners are:

$$(V_{zz})_{\alpha+\beta} = (-2A^2 + 16B^2 - 2C^2)/7 \tag{9}$$

and

$$(V_{xx} - V_{yy})_{\alpha+\beta} = 8\sqrt{3}\,(AC)/7\,. \tag{10}$$

The contribution of states within 2000 cm^{-1} of the ground state has been included in the total value of electric field gradients

$$(V_{zz})_T = \sum_N (V_{zz})_{N(\alpha+\beta)} \cdot \exp\left(-E_N/kT\right) \tag{11}$$

and similarly for $(V_{xx} - V_{yy})_T$.

In a rhombic field, the magnitude of the splitting of the Mössbauer resonance of Fe^{57} due to interaction of the electric field gradient with the excited state nuclear quadrupole moment is:

$$\Delta E = \tfrac{1}{2}\, eQ(q^2 + \eta^2 q^2/3)^{\frac{1}{2}} \tag{12}$$

where

$q = (V_{zz}) = (1 - R)\, q_{\text{val}} + (1 - \gamma)\, q_{\text{lat}}$,

$\eta q = (V_{xx} - V_{yy}) = (1 - R)\, n_{\text{val}}\, q_{\text{val}} + (1 - \gamma)\, n_{\text{lat}}\, q_{\text{lat}}$,

$q_{\text{lat}} = 14\,\mu/3e\,\langle r^2\rangle$ = lattice contribution to the z component of electric field gradient,

$n_{\text{lat}}\, q_{\text{lat}} = 7R/e\,\langle r^2\rangle$ = lattice contribution to the difference in x and y components of electric field gradient,

$q_{\text{val}} = (V_{zz})_T\,\langle r^{-3}\rangle$, where $(V_{zz})_T\,\langle r^{-3}\rangle$ is the sum of the expectation values of the $(V_{zz})_T$ operator $\langle(3z^2 - r^2)/r^5\rangle$ for all states within 2000 cm^{-1} of the ground state,

and $n_{\text{val}}\, q_{\text{val}}$ is the same sum for the $(V_{xx} - V_{yy})$ operator. $(1 - \gamma)$ and $(1 - R)$ are Sternheimer antishielding factors [7]. We have used the following values of the shielding factors and average values of radial distances:

$(1 - \gamma) = 10.14$ [7]; $\langle r^2\rangle = \langle r_0^2\rangle = 1.4$ a.u. [8]; $(1 - R)\langle r^{-3}\rangle = 3.3 - 4.0$ a.u. [8].

Substituting these values and expressions into the total expression for q and ηq and converting to units such that q and ηq are in esu/cm^3, ΔE in mm/sec and Q in Barns we obtain:

$$q = 4.982 \times 10^{11}\,\mu - 1.297 \times 10^{16}\,(V_{zz})_t \tag{13}$$

$$\eta q = 1.047 \times 10^{12}\, R - 1.297 \times 10^{16}\,(V_{zz} - V_{yy})_t \tag{14}$$

$$\Delta E = 3.077 \times 10^{-15}\, Q(q^2 + \eta^2 q^2/3)^{\frac{1}{2}} = CQ\,. \tag{15}$$

We see then that the total value of the electric field gradient is dependent on the rhombic field strength, the tetragonal field strength and the expectation values of the valence contribution to the field gradient. These latter quantities are calculated with three component eigenfunctions whose coefficients of mixing also depend on these field parameters.

Eigenfunctions and eigenvalues were obtained from the solution of the 3 × 3 spin-orbit rhombic-field matrix as a function of the parameters μ, R and δ using a matrix diagonalization program written for the Burroughs 5500. From these resulting eigenfunctions and eigenvalues, the magnetic field energies, electric field gradients and magnetic moments were also calculated, as a function of the field and spin-orbit coupling parameters by an expectation value subroutine which was added to the matrix diagonalization program for the Burroughs 5500.

C. Results

As mentioned, single crystal electron spin resonance of one low spin compound, the ferric hemoglobin azide, has been done and three distinct g values obtained.

The effective magnetic moment of this compound has also been measured and is reported to have a value of 2.35 – 2.84 [*1*, *2*, *3*] Bohr magnetons. The quadrupole splitting of the Mössbauer resonance has also been observed to be 2.00 – 2.30 mm/sec [*6*, *9*].

GRIFFITH [*10*] has used the measured g values of the azide to calculate the coefficients A, B and C of the ground state wave function. With the restriction of taking A, B and C real and $\sqrt{2}\,A + B$ positive, he obtains values of $A = .842$, $B = .128$ and $C = .525$. For the special case of letting R and μ be proportional to the spin-orbit coupling constant, these three values of the coefficients correspond to a value of $R = -2.26\,\delta$ and $\mu = 3.32\,\delta$. The exact physical significance of making the field parameters proportional to the spin-orbit coupling is not clear. There does not seem to be any physical necessity for so doing. Mathematically, of course, it has the effect of allowing the spin-orbit coupling to factor out of the 3×3 matrix. Hence the eigenfunctions are independent of δ while the eigenvalues are proportional to it.

We have repeated this calculation, solved the 3×3 matrix with the above relationship for R and μ and for two specific values of δ. The zero field splitting, i.e. relative energy intervals between the three low spin ground state components, at the two values of $\delta = 300$ and 420, the free ion value, are given in Tab. 9.

Table 9. *Zero field splitting*[a] *and electric field gradients for field parameters* $R = -2.26\,\delta$, $\mu = 3.32\delta$

δ	ΔE_1	ΔE_2	$(V_{zz})_T$	$(V_{xx} - V_{yy})_T$
300	745	1432	−.2433	−.8740
420	1043	2005	−.2433	−.8740

[a] Energy unit is cm^{-1}.

This relationship leads us then to the notion that the amount of function mixing is independent of the value of spin-orbit coupling, which is true only for this special restraint on the field parameters. This restraint also has the effect of fixing the ratio of μ/R at 3.32/2.26 which cannot be a general property of all types of rhombic distortions. In fact, it seems that a rhombic distortion with $|E\varepsilon|$ cubic symmetry can lead to a fixed ratio of R/μ since a tetragonal distortion has $|E\theta|$ symmetry. The matrix elements of two operators belonging to a different component of the same representation can be factored into a different coupling coefficient term for each operator multiplying the same reduced matrix element. Hence there is the possibility of a proportionality between the two. However for a rhombic distortion belonging to the cubic representation T_2, another common case, such proportionality is not in general obtained [*11*].

The negative value of R implies that the d_{xz} orbital energy lies below the d_{yz}. GRIFFITH in his original paper [*10*] notes this not very obvious result and makes some attempt to explain it by invoking bonding possibilities. Since that time, this result has been discussed on several occasions [*3*, *12*], with some elaboration and alteration of the original explanation for the ordering of the d_{xz} and d_{yz} orbitals. While there seems to be clear evidence that the d_{xy} orbital lies lower than either of these, i.e. μ is positive [*12*], there is not to this date any definite explanation for the order of the d_{yz} and d_{xz} orbitals. Before any more models of the bonding in this complex are made based on this ordering, we thought it reasonable at this point to examine the necessity of using a negative R and the restraint that the spin-orbit coupling parameter and field parameters need be proportional.

In order to investigate this effect, we have allowed R to be positive which means that the d_{yz} orbital energy lies below the d_{xz} orbital while keeping μ positive, i.e. the d_{xy} energy is lowest. We have considered sets of μ and R with each in the range 250 – 3000 cm^{-1} (i.e. R, $\mu = 250$, 500, 1000, 2000 and 3000 cm^{-1}) together with two values of δ, 300 and 420 cm^{-1}, and calculated fifty sets of three eigenfunctions and eigenvalues.

The first question to be answered was whether any results with a positive value of R gave g values close to the experimental ones. The answer to that is affirmative.

Table 10. *Calculated g values as a function of rhombic and tetragonal field strength*[a]

μ	R	250	500	1000	200	3000
250	g_x	0.513	.316	1.21	1.74	1.87
	g_y	2.30	2.71	2.84	2.63	2.47
	g_z	2.80	2.71	2.53	2.33	2.24
500	g_x	.098	.671	1.39	1.79	1.89
	g_y	2.02	2.46	2.65	2.52	2.41
	g_z	3.19	2.98	2.65	2.36	2.25
1000	g_x	.338	1.02	1.57	1.85	1.92
	g_y	1.68	2.16	2.41	2.39	2.32
	g_z	3.51	3.19	2.74	2.39	2.26
2000	g_x	.657	1.26	1.70 (1.72)	1.89	1.94
	g_y	1.40	1.90	2.20 (2.20)	2.25	2.23
	g_z	3.66	3.27	2.78 (2.80)	2.41	2.27
3000	g_x	.777	1.35	1.75	1.91	1.95
	g_y	1.28	1.79	2.10	2.18	2.17
	g_z	3.70	3.30	2.79	2.41	2.28

---

[a] $\delta = 420$. Units are cm^{-1}. Experimental g values in parenthesis.

From the variation of g values with R positive we conclude that the g values are fairly sensitive to the magnitude of R and that an $R = 1000$ is definitively selected from the range of 250 – 3000 considered. The magnitude of R determines the extent of mixing of the E'' and E' states and hence the relative magnitudes of the A and C coefficients. The results are also sensitive to the value of μ. This parameter determines to a large extent the mixing of the B_2 state into the ground state. The g variation with μ and R for $\delta = 420$ cm^{-1} is shown in Tab. 10. Results with $\delta = 300$ are not very different. Fairly reasonable agreement with experiment is obtained with $R = 1000$, for $\mu = 1000$, 2000 and 3000, for both $\delta = 300$ and 420 cm^{-1}. The closest agreement which is within experimental accuracy however is obtained for $R = 1000$, $\mu = 2000$ and $\delta = 420$ cm^{-1}.

Tab. 11 summarizes the differences in the g values obtained from the best assignment with $+R$ varied freely and $-R$ restrained to proportionality with

δ and μ. We see from this table that a somewhat better fit to g values is obtained from a $+ R$ assignment. We also see that the value of g is not very sensitive to the sign of R. The reason for this appears to be the following: allowing R to be positive removes the restriction that $\sqrt{2}\, A + B$ be positive. A is in fact negative. It is also much larger than B which keeps the same sign. If we examine the effect this sign change has on the various components of g, we find that it does not affect g_z at all which depends on A^2. It would in general affect g_x and g_y. However for the case of $A \gg B$, which is true here, a small quantity B added or subtracted to A makes little difference. It is this small difference that allows a somewhat better assignment in one case than the other. We conclude that from a g value assignment alone, a $- R$ assignment is not necessary and in fact a $+ R$ assignment fits the data somewhat better.

Table 11. *Summary of calculated results obtained for $-R$- and $+R$-assignment*

	$-R$-assignment[a]	$+R$-assignment[b]
R	-950	$+1000$
μ	$+1400$	$+2000$
δ	420	420
A	.842	$-.837$
B	.128	$+.097$
C	.525	$+.539$
ΔE_1 [cm^{-1}]	1043	1091.0
ΔE_2 [cm^{-1}]	962	1517
ΔE [cm^{-1}]	2005	2608
g_x	1.62	1.70
g_y	2.30	2.20
g_z	(2.80)	2.78
V_{zz}(val)	$-.2433$	$-.2616$
$V_{xx} - V_{yy}$ (val)	$-.8740$	$-.8926$
C	18.28 – 18.03	20.4 – 22.1
Q [Barns]	.126 – .127	.104 – .113
μ_{eff} [Bohr mag]	2.28	2.29

---

[a] Best values of g with restraint: $R = -2.26\,\delta$, $\mu = 3.32\,\delta$.

[b] Best values of g allowing free variation of R, μ and δ.

In order to further describe the system, we have calculated the values of the electric field gradients obtained from both $- R$ and $+ R$ values. For the field parameters in the form $R = -2.26\,\delta$, $\mu = 3.32\,\delta$, the valence contributions to the electric field gradient components are independent of δ. These values of $(V_{zz})_T$ and $(V_{xx} - V_{yy})_T$ are given in Tab. 9 and correspond to total valence contributions of $q_{\text{val}} = -2.60 \times 10^{15}$ esu/cm^3 and $\eta_{\text{val}}\, q_{\text{val}} = -9.35 \times 10^{15}$ esu/cm^3. The lattice contribution to V_{zz} with a $+ \mu$ subtracts from the valence contribution and the lattice contribution to $(V_{xx} - V_{yy})$ with a negative R adds to the valence contribution. The numerical value of the lattice contribution depends on the value selected for the spin-orbit coupling parameter. These are given in Tab. 12 for three values of δ. Comparing them to the two valence contributions given above we see that the lattice makes a contribution to V_{zz} of 28 to 6% and to the $(V_{xx} - V_{yy})$ component of 11 to 2.5%. The quantity C, the total numerical factor multiplying Q, i.e. $\Delta E = CQ$, is also given in Tab. 12. We see that even though the lattice contribution is greatly affected by the field values, since it is a small part of the total electric field gradient, the value of the total numerical constant C is not much affected by the change in this small contribution. Unfortunately the value of Q is unknown. The most that can be done with the final relationship is to use the observed value of ΔE and the calculated values of the electric field gradient components, i.e. C, to calculate a value of Q. The value of Q obtained is listed in Tab. 12 for a measured value of $\Delta E = 2.30$ mm/sec [*6*]. This is to be compared with values Q calculated for other ferric systems. ΔE has been measured and q calculated for Fe_2O_3 and ferric ion in rare earth garnets [*13*—*16*]. In these high spin systems the valence contribution was assumed zero. A range of Q values was obtained of .185 — .487. We see then that with this low spin calculation we are on the low side of results from other calculations. This range of C and Q values from the $-R$ assignment are listed again in Tab. 11 where they are compared with those obtained from the $+R$ assignment.

Table 12. *Electric field gradient and predicted value of Q as a function of spin-orbit coupling strength*

δ	420	300	100
$q_{\text{lat}} \times 10^{15}$	0.695	0.496	0.165
$\eta q_{\text{lat}} \times 10^{15}$	0.993	0.709	0.236
C^{a}	18.03	18.06	18.28
Q [Barns] $(\Delta E_{\text{exp}}/C)^{b}$	0.127	0.127	0.126

[a] C is defined in Eq. (15). $\Delta E = CQ$.
[b] $\Delta E_{\text{exp}} = 2.30$ mm/sec for the ferrihemoglobin azide [*6*].

Table 13. *Electric field gradients: variation with μ and δ for R best fit to g values* ($R = 1000$ cm^{-1})

μ	g_x	g_y	g_z	(V_{zz})	$(V_{xx} - V_{yy})$
			$\delta = 420$ cm^{-1}		
1000	1.57	2.41	2.74	−.2225	−.8718
2000	1.70	2.20	2.78	−.2616	−.8926
3000	1.75	2.10	2.79	−.2732	−.8999
			$\delta = 300$ cm^{-1}		
1000	1.78	2.33	2.57	−.2541	−.9285
2000	1.85	2.17	2.58	−.2540	−.9390
3000	1.87	2.10	2.59	−.2797	−.9424

The valence contribution to each component of the electric field gradient was also calculated for each set of eigenfunctions obtained with a $+R$ assignment of rhombic field parameters and the free variation of μ and δ. These values for $R = 1000$ cm^{-1} and $\delta = 300$, 420 cm^{-1} as a function of μ are given in Tab. 13. The total electric field gradient, the factor C, calculated for the best fit to the g values, i.e. $R = 1000$, $\mu = 2000$ and $\delta = 420$ cm^{-1}, is given in Tab. 11 where it is compared to the value of C for the $-R$ assignment. From this table we see that the corresponding range of Q predicted for the $+R$ assignment is .104 — .113 Barns, even lower than the $-R$ prediction of .126 — .127. Again we see that the results are not terribly sensitive to the sign of R. If Q were known with great accuracy it might be possible to distinguish between these two assignments on this basis.

The effective magnetic moment of the ferric ion was also calculated from the spin-orbit mixed eigenfunctions, with the same values of R, μ and δ that fit the observed g values best. These are also given in Tab. 11. The zero field splitting is very large under these conditions, $\Delta E_1 > 1000\ \text{cm}^{-1}$. At room temperature this corresponds to a Boltzman factor of $\exp(-1000/kT) = 0.007$. Hence the excited state contribution to the effective magnetic moment is negligible. Using Eq. (8), the first and second order contributions to the effective magnetic moment were calculated. For the $+R$ assignment: $\mu^2_{\text{eff}} = 3.8675 + 1.4017 = 5.270$ and for the $-R$ assignment: $\mu^2_{\text{eff}} = 3.934 + 1.302 = 5.236$ leading to the values of effective magnetic moments of 2.29 and 2.38 Bohr magnetons respectively. The small difference is due to small differences in the values of g, in the off-diagonal matrix elements and in the zero-field splittings. These values of μ_{eff} are in good agreement with the experimental value of 2.35.

To summarize our low-spin rhombic field spin-orbit coupling results, we find: good agreement with experimental g values was obtained for assignment of parameters with R both positive and negative corresponding to d_{yz} lower and higher in energy respectively than the d_{xz} orbital, with and without the restraint of R proportional to δ. For $\delta = 420$, the actual numerical values of the $\pm R$ that best fit the data were quite similar, $R = -950$ and $\mu = 1400$ compared to $R = 1000$ and $\mu = 2000\ \text{cm}^{-1}$. Total electric field gradients calculated for the $+R$ assignments were somewhat larger than the $-R$, leading to a smaller predicted value of Q. In each case, the lattice contribution to V_{zz} was about 30% of the valence contribution and the lattice contribution to $(V_{xx} - V_{yy})$ was about 10% of the valence contribution. Good agreement with the measured magnetic susceptibility data was obtained with no appreciable difference between the calculated values. At this point then it might be concluded that this model for the low spin ground state is quite successful in explaining magnetic properties and less successful in unambiguously assigning a reasonable value of Q.

D. Comparison of High and Low Spin Results

The least successful result of our model for ferric ion in strong field complexes appears when one compares the high and low spin results obtained from it for values of the total electric field gradients. For the high spin system, the electric field gradient calculated for the parameters that gave good agreement with the ESR data, yielded total values of Q in the range .275 – .505 Barns [*5*] when used with the experimental values of $\Delta E = 2$ mm/sec. These values are within the range of previous estimates of Q of .185 – .487 from other high spin ferric ion systems [*13*—*16*] and hence are not too discouraging.

Predicted values of the total nuclear quadrupole moment of Q of the excited state of the Fe^{57} nucleus were obtained from the ratio of the total electric field gradients calculated for a given iron complex and the observed splitting of the Mössbauer resonance of iron in the same complex, i.e.

$$Q_i = \Delta E_i(\exp) \,/\, C_i(\text{calc})\,.$$

Thus in comparing the values of Q predicted for a series of complexes one is actually comparing the ratio:

$$Q_1/Q_2 = \varDelta E_1/\varDelta E_2 \cdot C_2/C_1 .$$

C is defined by Eq. (15) and contains both the lattice and valence contributions to the tetragonal and rhombic terms of the electric field gradient. Our model is directly used to calculate what is essentially the expectation value of the angular portions of the field gradients. The expectation values of the radial integrals are taken from free ion calculations, as are the antishielding factors. Both of these, for a 23 electron atom, are quite difficult to calculate accurately. In the high spin system the lattice contribution is the dominant one. The valence contribution is 6 to 40% of it and goes to zero if excited states are excluded.

As long as we are comparing the values of Q obtained from different high spin ferric ion complexes and hence taking the ratio of essentially the lattice contributions, most of the arbitrariness due to the factor $(1-\gamma)\langle r^2\rangle$ multiplying the lattice contribution cancels. For the low spin system, the total electric field gradient has both a V_{zz} and $(V_{xx}-V_{yy})$ contribution to the observed splitting. Here, the valence contribution to both components is the dominant one and is fixed by the g value assignment. The lattice contribution varies from $6-28\%$ to V_{zz} and from $2-11\%$ to $(V_{xx}-V_{yy})$ for different reasonable values of field parameters. The value of Q obtained is .127. This is not too far from the values already predicted. However, in comparing high and low spin hemoglobin predictions for Q, we see that at best they are within a factor of 2 to one another. Since in the low spin case the valence contribution is the dominant one, the accuracy and validity of the factors $(1-R)\langle r^{-3}\rangle$ multiplying it are important. In the high spin case, with the lattice contribution dominant, it is the accuracy of the factor $(1-\gamma)\cdot\langle r^2\rangle$ which is important. The ratio of the total electric field gradients calculated for the low and high spin cases retain then, to a large extent, their dependence on the ratio of these factors. Thus the result obtained that a value of Q predicted from one system is twice the other contains in it not only the difficulties inherent in the calculation of the expectation values of the angular portion of the electric field gradients but also the rather significant difficulties of calculating accurate values for these different free atom properties. Since the agreement with experiment is least satisfactory for the one property calculated in which we do rely on parameters other than those directly involved in crystal field calculations, we may conclude that a rather significant part of our disagreement is probably due to these portions of the results. A better way perhaps to get at electric field gradients would be from a molecular orbital approach that did not involve the use of antishielding factors at all.

Hence, the crystal field model, assuming a strong field and including spin-orbit coupling, has been quite successful in explaining the properties of both high and low spin ferric ion in various hemoglobin derivatives. Magnetic susceptibilities and g values are accounted for consistently in going from one system to the other. However the predicted values of Q from the Mössbauer resonance quadrupole splitting of high and low spin ferriheme derivatives are at best within a factor of 2 of one another. This added ambiguity in comparing high and low spin results is probably due to the non-cancellation of the arbitrariness in the radial integrals and antishielding factors.

Acknowledgements. This work was supported by the Office of Naval Research, Contract Number *Nonr* 225(87). Reproduction in whole or in part is permitted for any purpose of the

United States Government. The invaluable assistance of Mr. KENNETH GUY in the writing of the matrix diagonalization and expectation value program is also gratefully acknowledged.

References

[1] SCHOFFA, G.: Advances chem. Physics **7**, 182 (1964).
[2] GEORGE, P., J. BEETLESTONE, and J. S. GRIFFITH: Rev. mod. Physics **36**, 441 (1964).
[3] INGRAM, D. J. E.: Paramagnetic resonance (W. Low Ed.), Volume II. New York: Academic Press 1963.
[4] HARRIS, G.: Work done under ONR contract Nonr 225(87), currently being prepared for publication.
[5] —, and M. WEISSBLUTH: Physic. Rev., in press.
[6] LANG, G., and W. MARSHALL: Harwell Report HL 65/4265.
[7] STERNHEIMER, R. M.: Physic. Rev. **84**, 244 (1951); **95**, 736 (1954); **105**, 158 (1957).
[8] INGALLS, R.: Physic. Rev. **133**, 787 (1964).
FREEMAN, A. J., and R. E. WATSON: Physic. Rev. **131**, 2566 (1963).
[9] MALING, J.: Private communication.
[10] GRIFFITH, J. S.: Nature **180**, 30 (1957).
[11] MACFARLAND, R.: Private communication.
[12] GRIFFITH, J. S.: Biopolymers Symposia No. 1: Quantum aspects of polypeptides and polynuclestides (M. WEISSBLUTH, Ed.). New York: Interscience Publishers 1964.
[13] BURNS, G.: Physic. Rev. **124**, 524 (1961).
[14] ALFF, C., and G. K. WERTHEIM: Physic. Rev. **122**, 1414 (1961).
[15] BUCHANAN, D. N. E., and G. K. WERTHEIM: The Mössbauer Effect, edited by C. M. J. COMPTON, and A. A. SCHOEN, p. 130. New York: Wiley 1962.
[16] NICHOLSON, W. J., and G. BURNS: Physic. Rev. **133**, 1568 (1964).

Dr. GILDA HARRIS
Pomona College
Department of Physics
Claremont, California, USA